Possible Origin of the Absence of Magnetic Order in LiOsO₃: Spin–Orbit Coupling Controlled Ground State

Yu Zhang, Jijun Gong, Chuanfu Li, Lin Lin, Zhibo Yan, Shuai Dong,* and Jun-Ming Liu

LiOsO₃ is the first experimentally confirmed polar metal with ferroelectric-like distortion. One puzzling experimental fact is its paramagnetic state down to very low temperature with negligible magnetic moment, which is anomalous considering its $5d^3$ electron configuration since other osmium oxides (e.g., NaOsO₃) with $5d^3$ Os ions are magnetic. Here the magnetic and electronic properties of LiOsO₃ are re-investigated carefully using the first-principles density functional theory. The calculations reveal that the magnetic state of LiOsO₃ can be completely suppressed by the spin–orbit coupling. The subtle balance between significant spin–orbit coupling and weak Hubbard U of $5d$ electrons can explain both the nonmagnetic LiOsO₃ and magnetic NaOsO₃. This work provides a reasonable understanding of the long-standing puzzle of magnetism in some osmium oxides.

Correlated electron systems with appreciable Coulomb repulsion are one of the most attractive platforms for accessing a series of emerging physical properties such as metal-insulator transition (MIT), superconductivity, colossal magnetoresistance, multiferroicity, and so on, which are often technologically useful. Such a Coulomb repulsion is usually characterized by the on-site Hubbard U. On the other hand, spin–orbit coupling (SOC) in condensed matters is becoming highly concerned, evidenced within a lot of emergent quantum materials such as topological insulators, Weyl semi-metals, and Kitaev systems,[1–4] where SOC can be the core ingredient of physics underlying their novel physical phenomena. On one hand, SOC can be strong for heavy ions, and even comparable to U for $5d$ electrons. For example, SOC is believed to play a

decisive role in determining the unconventional properties in those $5d^5$ transition metal oxides,[5] such as the $J_{\text{eff}} = 1/2$ Mott state for iridates (Ir⁴⁺).[6] On the other hand, the wavefunctions of $5d$ electrons are more extended than those of $3d$ and $4d$ electrons, which effectively reduces the on-site Coulomb repulsion U. Therefore, the competitive and/or cooperative effect of SOC plus Coulomb repulsion provide a unique playground for novel $5d$ electronic properties.

Here we consider a specific $5d$ perovskite system: LiOsO₃, which is known as the first experimentally confirmed polar metal with ferroelectric-like structural transition,[7] as predicted by Anderson and Blount.[8] Certainly, the major concern with such an unusual ferroelectric-like metallic state is not only the potential functionality but more importantly possible competition and coupling between the ferroelectricity and metallicity which are usually mutually exclusive.

A well-known but yet unsolved puzzling issue of LiOsO₃ is its magnetic ground state. In LiOsO₃, each Os ion is surrounded by an oxygen octahedron, which splits Os's $5d$ orbitals into the t_{2g} and e_g sectors by the crystalline field. In the ideal limit, the three $5d$ electrons of Os⁵⁺ ion will occupy the t_{2g} orbitals in the half filling manner. If the SOC effect is negligible, the half-filled t_{2g} orbitals will lead to a total spin angular moment $S = 3/2$ and a total orbital angular moments $L = 0$, driven by the Hund's rule. Thus, the ideal magnetic moment should be $3\,\mu_B$/Os. Indeed, experiments show that most osmium oxides, e.g., NaOsO₃, Cd₂Os₂O₇, and Ba₂YOsO₆, have magnetic ground states, and their Curie/Nèel temperatures are $\approx$69–410 K.[9–11] However, although LiOsO₃ has a simple perovskite crystal structure and $5d^3$ electron configuration similar to NaOsO₃, LiOsO₃ was experimentally found to show no any magnetic ordering even down to low temperature ($\approx$2 K).[7] Later, a muon-spin relaxation (μSR) experiments also revealed the absence of magnetic order in LiOsO₃ down to 0.08 K.[12]

There are several possible theoretical explanation for the absence of magnetic state in LiOsO₃. However, these theoretical proposals are rather confusing and often contradicting. For example, in ref. [13], the local density approximate (LDA) + dynamical mean field theory (DMFT) calculations give a nonmagnetic (NM) to G-type antiferromagnetic (G-AFM) transition at ($U = 1.25$ eV, $J_H = 0.1875$ eV) or ($U = 0.7$ eV, $J_H = 0.21$ eV), while the LSDA + U calculations in ref. [14] report

Y. Zhang, J. J. Gong, C. F. Li, Dr. L. Lin, Dr. Z. B. Yan, Prof. J.-M. Liu
Laboratory of Solid State Microstructures
Nanjing University
Nanjing 210093, China

Prof. S. Dong
School of Physics
Southeast University
Nanjing 211189, China
E-mail: sdong@seu.edu.cn

Prof. J.-M. Liu
Institute for Advanced Materials
Hubei Normal University
Huangshi 435002, China

The ORCID identification number(s) for the author(s) of this article can be found under https://doi.org/10.1002/pssr.201800396.

that the stable ground state should be a slater-type G-AFM insulator. In ref. [15], ($U = 2.3$ eV, $J_H = 0.345$ eV) are adopted in the LDA + DMFT calculation which can lead to a large local moment ($\approx 2.5\,\mu_B$/Os).[13] Then a crucial question is what are the proper values of U (and J_H) for $LiOsO_3$, which are decisive for the ground state in the first-principles calculations. The resonant inelastic X-ray scattering (RIXS) experimental suggestion for J_H is about 0.3 eV for osmium oxides.[10,16,17] If so, the ground state should be magnetic in both LSDA + U and LDA + DMFT calculations. Then the paramagnetism down to extreme low temperature remains a puzzle. Although the quantum fluctuation is expected to suppress the magnetic order and lead to so-called spin liquid state in some materials, here the large spin number $S = 3/2$ seems to be not a proper candidate for the strong quantum fluctuation.

In this work, we will carefully re-investigate the electronic structure and magnetic ground state of $LiOsO_3$ as well as $NaOsO_3$ based on the density functional theory (DFT) calculations. The combined effect of SOC plus U allows a comprehensive identification of the role of SOC, which has been somehow ignored in earlier studies.

Computation Methodology: The DFT calculations are performed using the pseudo-potential plane wave method as implemented in Vienna Ab initio Simulation Package (VASP).[18–20] The electron interactions are described using the Perdew–Burke–Ernzerhof (PBE) of the generalized gradient approximation (GGA).[21] The projected augmented wave (PAW)[22] pseudo-potentials with a 500 eV plane-wave cutoff are used, including three valence electrons for Li ($1s^2 2s^1$), nine for Na ($2s^2 2p^6 3s^1$), fourteen for Os ($5p^6 6s^2 5d^6$), and six for O ($2s^2 2p^4$).

To investigate the combined effect of on-site Coulomb potential U and SOC, we perform the GGA + U and GGA + U + SOC calculations in details on a set of assigned magnetic structures, so that the interplay of U and SOC can be clarified.

The low temperature structures of $LiOsO_3$ and $NaOsO_3$ are shown in **Figure 1**(a) and (b), respectively. Starting from the experimental structures, the lattice constants and all atomic coordinates are fully relaxed within the initial space groups, until the Hellman–Feynman forces on every atom are converged to less than 1.0 meV $Å^{-1}$. To accommodate the magnetic structure, $2 \times 2 \times 2$ supercell of $LiOsO_3$ containing 80 atoms to build various types of antiferromagnetic (AFM) orders. A $20 \times 20 \times 20$ mesh for the unit cell of $LiOsO_3$, a $7 \times 7 \times 7$ mesh for the supercell of $LiOsO_3$, and a $13 \times 13 \times 13$ mesh for the unit cell of $NaOsO_3$, are used for the Brillouin-zone sampling.

Here four magnetic ordered structures: A-type AFM (A-AFM) order, C-type AFM (C-AFM) order, G-AFM order, ferromagnetic (FM) order are considered in the present calculations, plus the NM state. The three AFM orders are sketched in **Figure 2**(a–c).

Results and Discussion: To solve the aforementioned confusing theoretical results, it is necessary to clarify the methods of + U in the first-principles calculations. Taking the most used VASP code for example, there are three choices of + U: a) LDAUTYPE = 1: the rotationally invariant LSDA + U introduced by Liechtenstein et al.[23]; b) LDAUTYPE = 2: the simplified (rotationally invariant) approach to the LSDA + U, introduced by Dudarev et al.[24]; c) LDAUTYPE = 4: LDA + U. The LDAUTYPE = 2 is the most used (default) choice, which only needs a parameter
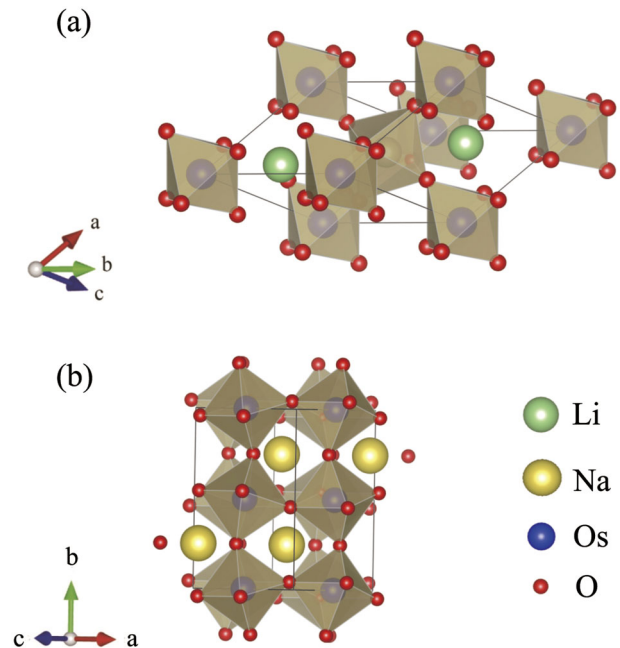

Figure 1. Crystal structure of (a) $LiOsO_3$ and (b) $NaOsO_3$. The green, yellow, blue, and red balls are Li, Na, Os, and O ions.

$U_{eff} = U - J$. For the LSDA calculation (LDAUTYPE = 1 and 2), the exchange splitting, e.g., the effect of J_H, has already (partially) included, even without U. In other words, the U and J_H in these two choices are not the naked ones as used in the Hubbard
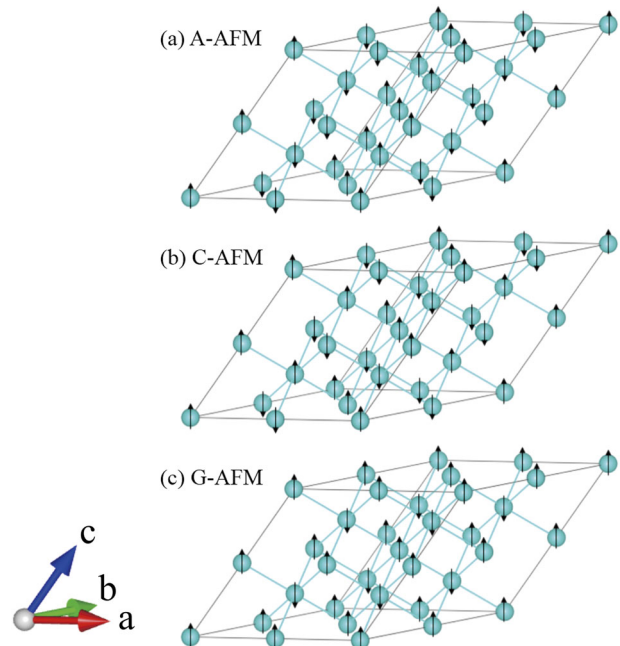

Figure 2. Schematic of three candidate antiferromagnetic orders for $LiOsO_3$. a) A-AFM, b) C-AFM, c) G-AFM in the $2 \times 2 \times 2$ supercell. Only Os ions are shown and the arrows represent the signs of magnetic moments.

models, or DMFT calculations, or RIXS experiments, but significantly reduced. Instead, the rarely used LDA + U (LDAUTYPE = 4) choice can give naked U and J_H to compare between the DFT, model, DMFT, as well as RIXS experiment.

First, the LDA + U (LDAUTYPE = 4) choice is tested for LiOsO$_3$ and the results are shown in **Figure 3**. Two cases of J/U (=0.15 and 0.3) are considered for example. The lattice constant a is a little larger than the experimental one, and gradually increases with U (Figure 3(a)). It is well known that GGA will systematically and slightly overestimate the lattice constants. Despite this point, our result agrees with the experimental value, especially in the low U region. The G-AFM state is the lowest energy one among all magnetic candidates. Thus, the energy difference between G-AFM and NM state is shown Figure 3(b), which becomes negligible in the low U region, e.g., $U \leq 0.9$ eV for $J/U = 0.3$ or $U \leq 1.3$ eV for $J/U = 0.15$. Not surprisingly, the energy degeneration in the low U region is due to the quenching of local moment of Os, although the critical value of Us for zero local moment is a little bit lower for 0.2–0.3 eV, as shown in Figure 3(c). With increasing U, the MIT occurs almost accompanying the NM-G-AFM transition (Figure 3(d)), with slightly shift of critical U for 0.1–0.2 eV higher. These results obtained in our LDA + U calculation agrees with previous LDA + DMFT results.

By calculating more points of J and U, a phase diagram can be sketched as **Figure 4**. In addition, the calculation with SOC is
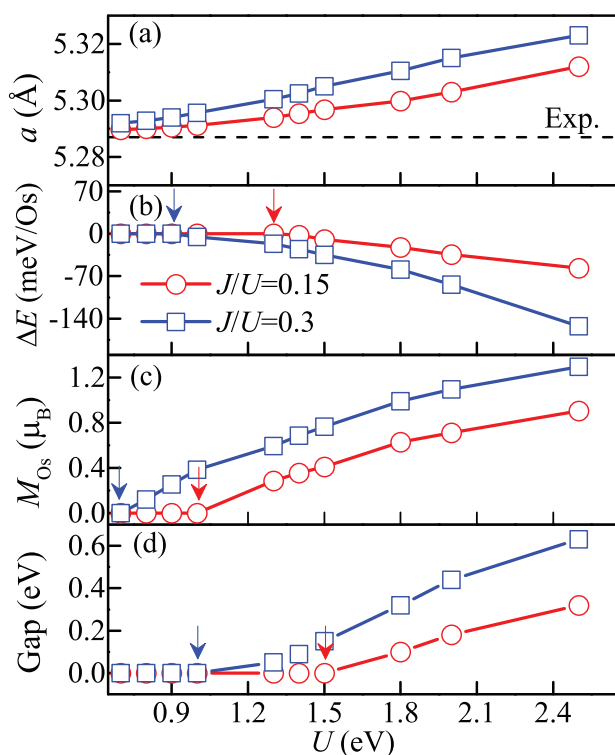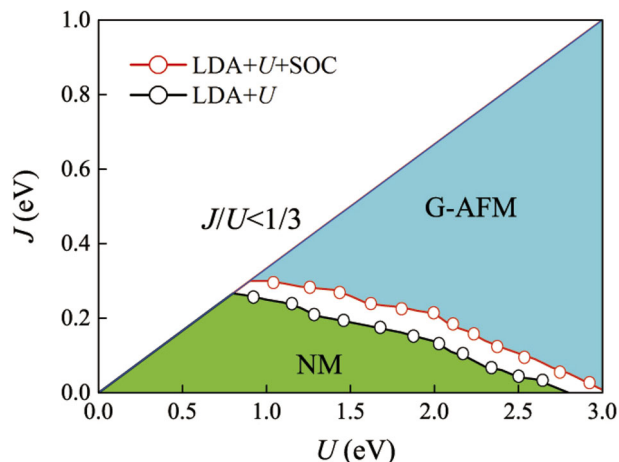

Figure 4. The magnetic phase diagram of LiOsO$_3$ calculated by LDA + U and LDA + U + SOC. Physically, J/U should be less than 1/3. The phase boundary between NM and G-AFM is shifted to higher U and J side by SOC.

also performed, which can slightly shift the NM-G-AFM boundary to larger U and J side. As expected, the NM state exists in the low U and low J region. Taking the experimental value of $J_H \approx 0.3$ eV for reference, the ground state is probably located at the boundary between NM and G-AFM state, with zero or very small local moment (<0.25 μ_B/Os), instead of large local moment ($\approx 2.5 \mu_B$/Os) obtained in ref. [15]. Thus it is probably that LiOsO$_3$ is indeed NM with almost zero or very small local moment, which can properly understand the paramagnetism down to very low temperatures.
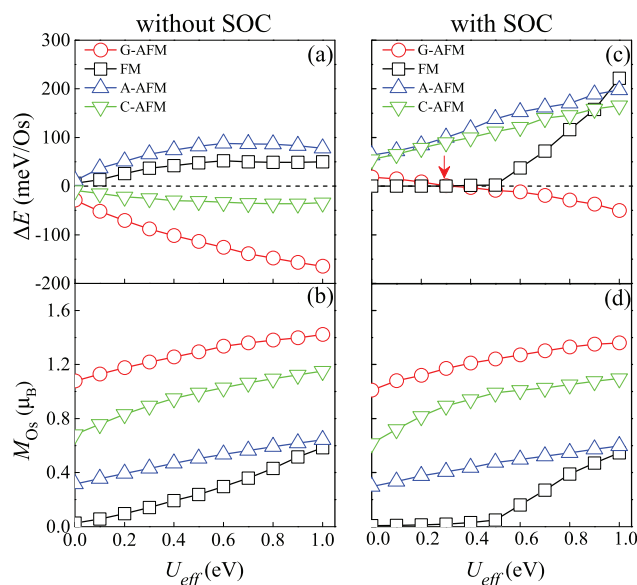

Figure 3. Results of LDA + U calculations for LiOsO$_3$ as a function of U. Two ratios of J/U are considered. a) The optimized lattice constant in G-AFM state. b) The energy difference between G-AFM state and NM state ($\Delta E = E_{G\text{-}AFM} - E_{NM}$). c) The magnetic moment of Os ion. d) The energy gap of LiOsO$_3$ in G-AFM state.

Figure 5. Results of LSDA + U and LSDA + U + SOC calculations for LiOsO$_3$ as a function of U_{eff}. a,b) Without SOC. c,d) With SOC. a,c) The energy difference ΔE between the magnetic phases and NM one. b,d) The local Os^{5+} moment.
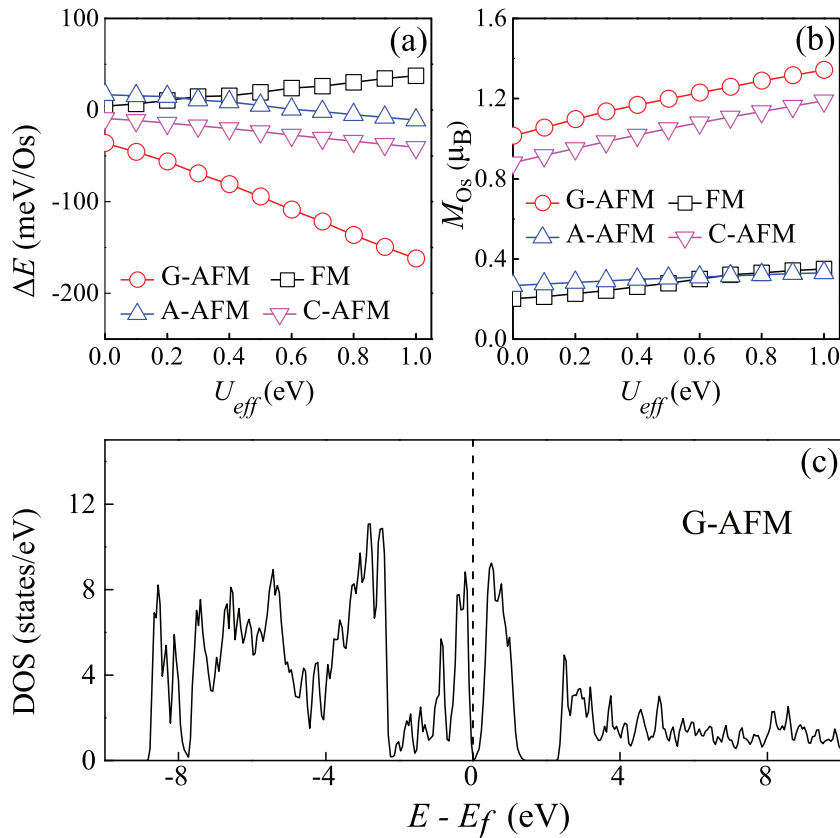
ADVANCED
SCIENCE NEWS
www.advancedsciencenews.com

physica
pss
status
solidi
rrl

www.pss-rapid.com

Figure 6. Results of LSDA + U + SOC calculations for NaOsO$_3$ as a function of U_{eff}. a) The energy difference ΔE between the magnetic phases and NM one. The G-AFM order is always the lowest one. b) The local Os^{5+} moment, which is always nonzero. c) The total density of states (DOS) of NaOsO$_3$ when $U_{eff} = 0$.

between spin-up and spin-down channels. In short, the SOC plays non-negligible role to obtain the NM ground state of LiOsO$_3$, at least in the LSDA + U calculation. Thus, the mostly used LSDA + U + SOC method can also describe the magnetic fact of LiOsO$_3$.

Then it is necessary to check this method in NaOsO$_3$, since a successful theoretical approach should be valid for various systems, at least for a family of materials. With the same LSDA + U method, our calculation confirms that the ground state for NaOsO$_3$ is G-AFM state, which is robust against the SOC, as summarized in **Figure 6**. This result is different from LiOsO$_3$, but agrees with the experimental factor, further confirming the LSDA + U (+SOC) method can describe these osmium oxides. For the moment of Os^{5+} in the G-AFM NaOsO$_3$ as a function of U_{eff}, the calculated value at $U_{eff} = 0$ eV is 1.01 μ_B and 1.38 μ_B at $U_{eff} = 1.0$ eV. It is noted that the measured moment for NaOsO$_3$ is about 1.0 μ_B, obtained from neutron scattering.[25] This implies convincingly $U_{eff} \approx 0$ eV in the LSDA + U calculations for NaOsO$_3$. And the density of states (DOS) of NaOsO$_3$ in G-AFM state with $U_{eff} = 0$ is shown in Figure 6(c), which is consistent with a pure Slater-type insulator, as confirmed in experiments.[25]

To better understand the contrastive magnetism of LiOsO$_3$ and NaOsO$_3$, the structural differences are shown in **Table 1**. It can be seen that the Os–O–Os network is more compact in LiOsO$_3$, with averagely shorter Os–O bonds and short distance between nearest-neighbor Os–Os. Thus, the hybridization between Os's 5d and O's 2p orbitals are more prominent in LiOsO$_3$ and the effective hopping between nearest-neighbor Os's 5d orbitals are larger. To further confirm this point,
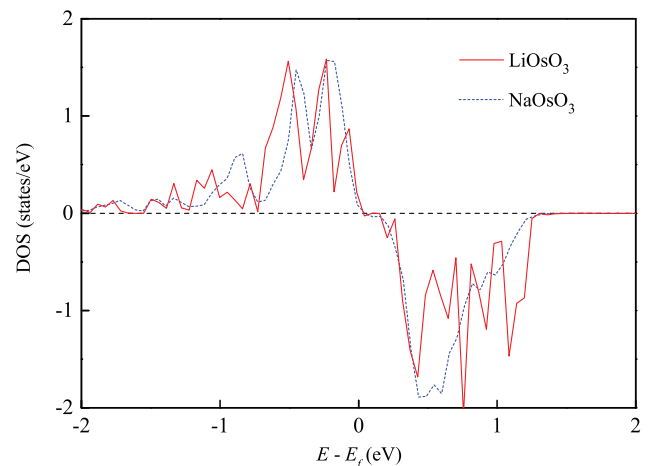
Then it is interesting to know whether the more commonly used LSDA + U method can correctly describe the nonmagnetism/magnetism of LiOsO$_3$. By setting LDAUTYPE = 2, the same processes have been done, whose results are summarized in **Figure 5**. Our LSDA + U results lead to magnetic ground state with large local moment (>1.1 μ_B/Os), which further increases with U_{eff}. So the LSDA + U calculation could not explain the experimental fact, then we consider the effect of SOC. By considering the SOC, the magnetic moment is reduced by residual orbital moment and the phase diagram is significantly changed. The NM state becomes the ground state in the low U_{eff} region (≤ 0.3 eV). The transition from NM to G-AFM is the first order with discontinuous jump of local moment. Physically, the SOC coupling (expressed as $\mathbf{L} \times \mathbf{S} = L^z S^z + (L^+ S^- + L^- S^+)/2$, where $\mathbf{L}$ and $\mathbf{S}$ are orbital and spin operators) can mix the spin-up and spin-down channels due to the raising and lowering operators L^+ and L^-, which would reduce the effective Hubbard repulsion

Table 1. Structural parameters of LiOsO$_3$ and NaOsO$_3$ calculated using LSDA with G-AFM order.

	LiOsO$_3$ (Å)	NaOsO$_3$ (Å)
Os–O bond length (average)	1.943	1.951
Nearest-neighbor Os–Os distance	3.654	3.788

Figure 7. The partial spin polarized DOS of a single spin-up Os in LiOsO$_3$ and NaOsO$_3$ in the G-AFM state calculated by LSDA. Here only the differences of spin-up and spin-down channel are shown.

the partial DOS's of each Os in $LiOsO_3$ and $NaOsO_3$ in the G-AFM state with $U_{eff} = 0$, are shown in **Figure 7**. As expected, the band width of $5d$ orbitals in $LiOsO_3$ is relatively wider than that in $NaOsO_3$. It is well known that the Mott transition (also the magnetic transition) of Hubbard model system depends on the subtle competition between the kinetic energy and Coulombic repulsion. The cases of Os^{5+} are just located around the critical point of Mott transition. The narrower $5d$ bands of $NaOsO_3$ is advantaged for magnetic moment, while the wider $5d$ bands of $LiOsO_3$ prefers the nonmagnetic metallic state.

Conclusion: The magnetic and electronic properties of $LiOsO_3$ and $NaOsO_3$ have been checked using first-principles methods. The long-standing puzzle regarding the paramagnetism of $LiOsO_3$ has been clarified. In our opinion, the local magnetic moment of Os^{5+} in $LiOsO_3$ can be zero or very small, due to the weak Hubbard U and indispensable SOC. The LSDA + U + SOC method can describe the magnetism of $LiOsO_3$, although the U used in LSDA is significantly reduced comparing with the value used in LDA + U or LDA + DMFT. In contrast, the magnetic ground state has been verified for $NaOsO_3$. The importance of SOC in determining the magnetic structure has already been proved in some other $5d^3$ osmium oxides such as Sr_2ScOsO_6 and $Cd_2Os_2O_7$.[16,26] Our work provides a uniform description for $LiOsO_3$ and other osmium oxides.

Conflict of Interest

The authors declare no conflict of interest.

[1] H. M. Guo, M. Franz, *Phys. Rev. Lett.* **2009**, *103*, 206805.
[2] D. Pesin, L. Balents, *Nat. Phys.* **2010**, *6*, 376.
[3] X. Wan, A. M. Turner, A. Vishwanath, S. Y. Savrasov, *Phys. Rev. B* **2011**, *83*, 205101.
[4] G. Jackeli, G. Khaliullin, *Phys. Rev. Lett.* **2009**, *102*, 017205.
[5] W. Witczak-Krempa, G. Chen, Y. B. Kim, L. Balents, *Annu. Rev. Condens. Matter Phys.* **2014**, *5*, 57.
[6] B. J. Kim, H. Jin, S. J. Moon, J. Y. Kim, B. G. Park, C. S. Leem, J. Yu, T. W. Noh, C. Kim, S. J. Oh, J. H. Park, V. Durairaj, G. Cao, E. Rotenberg, *Phys. Rev. Lett.* **2008**, *101*, 076402.
[7] Y. Shi, Y. Guo, X. Wang, A. J. Princep, D. Khalyavin, P. Manuel, Y. Michiue, A. Sato, K. Tsuda, S. Yu, M. Arai, Y. Shirako, M. Akaogi, N. Wang, K. Yamaura, A. T. Boothroyd, *Nat. Mater.* **2013**, *12*, 1024.
[8] P. W. Anderson, E. I. Blount, *Phys. Rev. Lett.* **1965**, *14*, 217.
[9] Y. G. Shi, Y. F. Guo, S. Yu, M. Arai, A. A. Belik, A. Sato, K. Yamaura, E. Takayama-Muromachi, H. F. Tian, H. X. Yang, J. Q. Li, T. Varga, J. F. Mitchell, S. Okamoto, *Phys. Rev. B* **2009**, *80*, 161104.
[10] S. Calder, J. G. Vale, N. A. Bogdanov, X. Liu, C. Donnerer, M. H. Upton, D. Casa, A. H. Said, M. D. Lumsden, Z. Zhao, J. Q. Yan, D. Mandrus, S. Nishimoto, J. van den Brink, J. P. Hill, D. F. McMorrow, A. D. Christianson, *Nat. Commun.* **2016**, *7*, 11651.
[11] E. Kermarrec, C. A. Marjerrison, C. M. Thompson, D. D. Maharaj, K. Levin, S. Kroeker, G. E. Granroth, R. Flacau, Z. Yamani, J. E. Greedan, B. D. Gaulin, *Phys. Rev. B* **2015**, *91*, 075133.
[12] F. K. K. Kirschner, F. Lang, F. L. Pratt, T. Lancaster, Y. Shi, Y. Guo, A. T. Boothroyd, S. J. Blundell, *JPS Conf. Proc.* **2018**, *21*, 011013.
[13] D. Puggioni, G. Giovannetti, M. Capone, J. M. Rondinelli, *Phys. Rev. Lett.* **2015**, *115*, 087202.
[14] C. He, Z. Ma, B.-Z. Sun, Q. Li, K. Wu, *Comput. Mater. Sci.* **2015**, *105*, 11.
[15] I. Lo Vecchio, G. Giovannetti, M. Autore, P. Di Pietro, A. Perucchi, J. He, K. Yamaura, M. Capone, S. Lupi, *Phys. Rev. B* **2016**, *93*, 161113.
[16] A. E. Taylor, R. Morrow, R. S. Fishman, S. Calder, A. I. Kolesnikov, M. D. Lumsden, P. M. Woodward, A. D. Christianson, *Phys. Rev. B* **2016**, *93*, 220408.
[17] S. Calder, J. G. Vale, N. Bogdanov, C. Donnerer, D. Pincini, M. Moretti Sala, X. Liu, M. H. Upton, D. Casa, Y. G. Shi, Y. Tsujimoto, K. Yamaura, J. P. Hill, J. van den Brink, D. F. McMorrow, A. D. Christianson, *Phys. Rev. B* **2017**, *95*, 020413.
[18] G. Kresse, J. Hafner, *Phys. Rev. B* **1993**, *47*, 558.
[19] G. Kresse, J. Furthmüller, *Comput. Mater. Sci.* **1996**, *6*, 15.
[20] G. Kresse, J. Furthmüller, *Phys. Rev. B* **1996**, *54*, 11169.
[21] J. P. Perdew, K. Burke, M. Ernzerhof, *Phys. Rev. Lett.* **1996**, *77*, 3865.
[22] P. E. Blöchl, *Phys. Rev. B* **1994**, *50*, 17953.
[23] A. I. Liechtenstein, V. I. Anisimov, J. Zaanen, *Phys. Rev. B* **1995**, *52*, R5467.
[24] S. L. Dudarev, G. A. Botton, S. Y. Savrasov, C. J. Humphreys, A. P. Sutton, *Phys. Rev. B* **1998**, *57*, 1505.
[25] S. Calder, V. O. Garlea, D. F. McMorrow, M. D. Lumsden, M. B. Stone, J. C. Lang, J. W. Kim, J. A. Schlueter, Y. G. Shi, K. Yamaura, Y. S. Sun, Y. Tsujimoto, A. D. Christianson, *Phys. Rev. Lett.* **2012**, *108*, 257209.
[26] H. Shinaoka, T. Miyake, S. Ishibashi, *Phys. Rev. Lett.* **2012**, *108*, 247204.